Int. J. Solids Structures Vol. 25, No. 10, pp. 1157–1175, 1989
Printed in Great Britain.

0020-7683/89 $3.00 + .00

AN INVESTIGATION OF THE FRACTURE PROCESS ZONE NEAR THE TIP OF A STEADILY PROPAGATING TENSILE CRACK

S. G. RUSSELL†
Department of Aerospace and Mechnical Engineering, University of Notre Dame, Notre Dame, IN 46556, U.S.A.

(*Received* 8 *October* 1987; *in revised form* 8 *September* 1988)

Abstract—This paper presents a model for the fracture process zone near the tip of a steadily propagating plane strain tensile crack. The material is assumed to be elastic-ideally plastic and completely incompressible. The macroscopic plastic deformation near the advancing crack tip is modeled by a slip element approach in which dislocations are continuously distributed over a planar region. The fracture process zone is modeled by a continuous distribution of dislocations collinear with the advancing crack tip. The results of the study reveal the influence of the fracture process zone on the slip line pattern within the crack tip plastic zone and on the elastic–plastic boundary. The fracture process zone model is also shown to give an accurate and physically reasonable estimate of the crack tip opening angle associated with continued ductile stable crack growth.

INTRODUCTION

In recent years, the elastic–plastic stress and deformation fields near the tip of a quasi-statically propagating tensile crack have been the subject of widespread theoretical attention. The motivation for this interest lies in the observation, e.g. Clark *et al.* (1978), that specimens of ductile metal can exhibit extensive stable crack growth prior to failure. The development of engineering analysis methods for flawed structures requires a sound foundation based upon a realistic fracture criterion for continued ductile crack growth.

Due to the mathematical complexity of the field equations governing the crack tip deformation processes, the most intense research efforts have focused on the asymptotic analysis of growing cracks under conditions of small-scale yielding. These studies, which are rigorously valid at vanishingly small distances from the crack tip, employ slip line methods similar to those used by Rice (1967) in the study of plastic deformation near a stationary crack. In one of the first of such works, Chitaley and McClintock (1971) obtained solutions for steady crack growth in anti-plane shear (mode III). They discovered the presence of both a primary plastic zone ahead of the propagating crack and a secondary plastic zone along the crack surfaces. Their study also identified the logarithmic strain singularity found by Rice (1968) in a preliminary investigation of steady state tensile crack growth (mode I). Slepyan (1974) reported similar findings in a study of plane strain shear crack growth (mode II) for a material obeying the Tresca yield condition. Rice and Sorenson (1978) performed an asymptotic analysis of a propagating tensile crack valid for general steady or unsteady growth regimes. Their analysis employed an assembly of crack tip plastic deformation sectors similar to the Prandtl slip line field associated with a stationary tensile crack. A logarithmic crack tip strain singularity was identified and a fracture criterion based upon the attainment of a critical crack opening displacement at a characteristic material distance behind the crack tip was proposed. Rice *et al.* (1980) later noted that the Prandtl slip line configuration contained a velocity discontinuity corresponding to negative plastic work, rendering it inappropriate as an asymptotic field for the growing crack. They proposed a modified asymptotic field containing a sector of elastic deformation that intervenes between the primary plastic zone ahead of the crack tip and the secondary plastic zone along the crack surfaces. An asymptotic analysis was then given for a material satisfying von Mises' yield condition under the assumption of elastic incompressibility at vanishingly

†Currently Senior Engineer, Northrop Corporation, Aircraft Division, 3853/82, 1 Northrop Avenue, Hawthorne, CA 90250, U.S.A.

small distances from the crack tip. The fracture criterion proposed in the earlier work of Rice and Sorenson (1978) was again found to be suitable for the growing tensile crack.

Rice (1982) generalized the results of previous asymptotic analyses for growing tensile and anti-plane shear cracks (modes I and III). He presented a formulation valid for anisotropic materials with arbitrary yield condition and associated flow rule. Detailed results for isotropic materials of the Huber–Mises type were recovered from the formulation, including an enumeration of the possible sectors of crack tip plastic deformation in a material with arbitrary Poisson's ratio. The detailed assembly of sectors into an asymptotic field for the growing plane strain tensile crack was given by Drugan *et al.* (1982). Their work contains an exact asymptotic analysis valid for isotropic materials with arbitrary Poisson's ratio and an approximate asymptotic analysis that gives details of the results presented in the earlier study of Rice *et al.* (1980). The exact asymptotic analysis identified a primary plastic zone containing three distinct sectors of deformation, a secondary plastic zone along the crack surfaces, and an intervening sector of elastic deformation between the primary and secondary plastic zones. Drugan (1986) has extended this work by presenting a higher-order asymptotic analysis that clarifies the radial dependence of the near-tip plastic deformation field associated with the growing plane strain tensile crack.

Recent analyses have expanded the scope of the previous work to include growing plane stress tensile cracks, growing plane stress shear cracks (mode II), and growing cracks in strain-hardening materials. Achenbach and Dunayevsky (1984) have employed the method of matched asymptotic expansions to obtain a complete solution for the normal strain component in the plane of a propagating plane stress tensile crack. Ponte Castañeda (1986) has given an asymptotic analysis for the growing plane stress shear crack, showing results that are similar in form to the two earlier studies of growing cracks in plane strain shear and anti-plane shear (Slepyan, 1974; Chitaley and McClintock, 1971). Finally Ponte Castañeda has presented two asymptotic analyses of crack growth in materials with strain-hardening. The first work (Ponte Castañeda, 1987a) gives general asymptotic solutions for steady crack growth in plane strain (modes I and II), plane stress (modes I and II), and anti-plane shear (mode III) for a material characterized by J_2 flow theory with linear strain-hardening. The second work (Ponte Castañeda, 1987b) presents asymptotic solutions for plane stress and plane strain steady tensile crack growth in a material characterized by J_2 deformation theory.

Numerical methods have been used to study the complete elastic-plastic stress and deformation fields associated with propagating tensile cracks. Sorenson (1979) and Dean and Hutchinson (1980) have presented finite element analyses of plane strain crack growth in a power-law hardening material. Sham (1983) has given a detailed finite element study of transient plane strain tensile crack growth in an elastic-ideally plastic material. Narasimhan *et al.* (1987a,b) have presented finite element analyses of plane stress tensile crack growth for both elastic-ideally plastic and strain-hardening materials. Other recent studies have employed microstructural models for the material to relate stable crack growth to the mechanism of microvoid growth and coalescence. Aravas and McMeeking (1985) have used large deformation finite element analysis to study the growth of a cylindrical void ahead of a blunting stationary crack. They employed a modified yield condition that reflects the growth of small-scale voids and the reduced load-carrying capacity of the porous material. Their results provide an estimate for the crack tip opening displacement required for fracture initiation in porous material that contains a single large-scale void near the crack tip. Needleman and Tvergaard (1987) have extended this work by considering the effect of an array of large-scale voids near the crack tip. They employed a modified constitutive relation that accounts for viscoplatic material behavior in the porous solid. The results of the finite element analysis are used to calculate the crack tip opening displacement required for fracture initiation and the tearing modulus associated with the early stages of crack growth.

The finite element analysis of growing cracks requires an extremely fine mesh for the calculation of accurate numerical results. In order to reduce computational effort, Denda (1983a) has formulated a planar slip element for steady crack growth based upon the theory of dislocations. His work contains the basic complex potential function solution for planar

slip in a plastically deforming rectangular element and its trailing wake. Although Denda's method is restricted to elastically incompressible, ideally plastic materials and requires the solution of a nonlinear system of equations, he has shown that it yields accurate results to the plane strain tensile crack growth problem on a rather coarse element mesh. It can also be combined with other dislocation-based approaches to crack tip plasticity to study more specialized problems. Recently, Denda (1986) has removed some of the restrictions on the use of the planar slip element with a new procedure that makes use of the Green's function representation of inelastic deformation by linear combinations of force dipoles or couples. This method has been shown by Denda and Lua (1986) to give good results for the steady state, plane strain tensile crack growth problem. Wu and Hui (1987a) have employed the fictitious body force method of Eshelby (1957) to develop a complex variable method for two-dimensional internal stress problems. They have considered various applications of their approach (Wu and Hui, 1987b), including problems of quasi-static, steady state crack growth for anti-plane shear and plane strain tensile loading.

In the present work, the results of an investigation of the fracture process zone near the tip of a steadily propagating plane strain tensile crack will be presented. The macroscopic plastic deformation near the advancing crack tip is modeled using the planar slip element method developed by Denda (1983a). The fracture process zone at the crack tip is represented as a continuous distribution of dislocations occupying the crack prolongation plane immediately ahead of the crack tip. The objective of the study is to clarify the fracture criterion for ductile stable crack growth proposed in the work of Rice and Sorenson (1978), Rice *et al.* (1980) and Rice (1982). These authors suggest that the characteristic material distance behind the advancing crack tip needed for the attainment of the critical crack opening displacement is related to the size of the fracture process zone. The quantitative analysis of the fracture process zone provided here will sharpen the existing fracture criterion.

The geometry of the problem is illustrated in Fig. 1, which shows a semi-infinite crack propagating steadily. The body containing the crack is of infinite extent in all directions, and the Cartesian coordinate axes are chosen so that the x_1-axis coincides with the advancing crack front. It is assumed that all transient effects subsequent to the initiation of crack growth have decayed, and that the crack has been propagating steadily for an indefinitely long period of time under the influence of a remote loading system that produces a constant mode I stress intensity factor K at the crack tip. Macroscopic plastic deformation extends over the planar region surrounding the crack tip and a fracture process zone occupies the segment of the x_1-axis immediately ahead of the crack tip. Small-scale yielding conditions are assumed to prevail near the growing crack. The dislocation configurations used to model the macroscopic plastic deformation and fracture process zone are invariant with respect to the coordinate system moving with the crack tip.

In what follows, descriptions of the planar slip element method and the fracture process zone model will be given. The method for combination of the two approaches through application of the yield condition for an elastically incompressible, ideally plastic material will be illustrated. Finally, the numerical solution for the problem will be discussed and the results of the study presented.

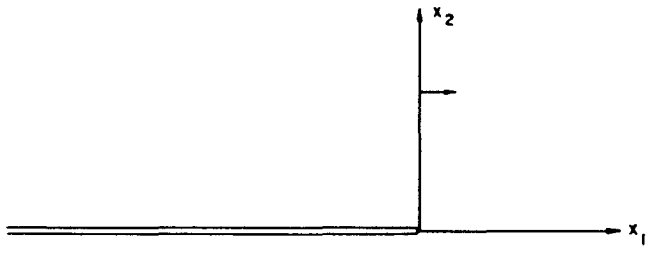

Fig. 1. Geometry of the steady tensile crack growth problem.

THE PLANAR SLIP ELEMENT METHOD

Denda (1983a) has shown that the stresses and displacements associated with planar slip over an isolated finite area can be calculated from the appropriate Muskhelishvili complex potential functions. The rationale for this approach derives from the fact that slip deformation can be represented as a continuous distribution of dislocation dipoles over a planar area. For the steady crack growth problem, consider a rectangular region R in the upper half of the x_1x_2-plane and its counterpart region $\bar{R}$ in the lower half-plane as illustrated in Fig. 2. Both regions consist of an active element plus a trailing wake of plastically deformed material. Employing a coordinate system that advances along with the steadily propagating crack, the plastic shear strain rate can be expressed as

$$\dot{\gamma}_p = -\frac{\partial \dot{\gamma}_p}{\partial x_1}, \tag{1}$$

where the dot denotes differentiation with respect to the monotonically increasing time parameter $t = a$ (a is the crack length). Assuming that the quantity $\dot{\gamma}_p$ is constant in the active element of regions R and $\bar{R}$, the spatial variation of plastic shear strain in the two regions is

$$\gamma_p(\xi) = \begin{cases} \dot{\gamma}_p(\xi_R - \xi) & \text{for } \xi_L \leqslant \xi \leqslant \xi_R, \\ \dot{\gamma}_p(\xi_R - \xi_L) & \text{for } -\infty < \xi < \xi_L. \end{cases} \tag{2}$$

This relation is used in the calculation of the complex potential functions for the inelastic slip deformation in regions R and $\bar{R}$. We shall refer to this pair of regions as a planar slip element. Due to the symmetry of mode I deformation with respect to the x_1-axis, the analysis of stress and displacement can be confined to the upper half-plane $x_2 > 0$.

Let us employ the complex notation $z = x_1 + ix_2$, where $i = (-1)^{1/2}$. For the case where the point z is outside the region R, the complex potential functions for the planar slip element are

$$\Phi(z) = \Phi_1^{ext}(z) + \Phi_2^{c}(z), \tag{3}$$

where

$$\Phi_1^{ext}(z) = \tfrac{1}{2} D\, e^{2i\alpha}\dot{\gamma}_p \sum_{m=1}^{4} (-1)^m (z-\zeta_m) ln(z-\zeta_m) + \tfrac{1}{2} D\, e^{-2i\alpha}\dot{\gamma}_p \sum_{m=1}^{4} (-1)^m (z-\bar{\zeta}_m) ln(z-\bar{\zeta}_m), \tag{4}$$

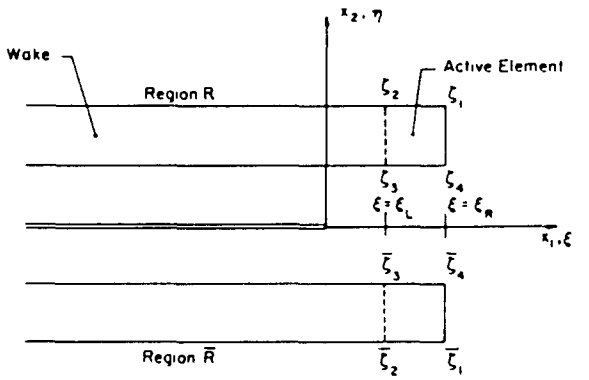

Fig. 2. Regions of deformation associated with the planar slip element.

$$\Phi_2^c(z) = -\tfrac{1}{2}D\,e^{2i\alpha}\gamma_p \sum_{m=1}^{4}(-1)^m\left[\frac{1}{z^{1/2}}(\tfrac{1}{3}\zeta_m^{3/2}+\zeta_m^{1/2}\bar{\zeta}_m)-2z^{1/2}\zeta_m^{1/2}\right.$$
$$\left.+(2z-\zeta_m-\bar{\zeta}_m)ln(z^{1/2}+\zeta_m^{1/2})\right]-\tfrac{1}{2}D\,e^{-2i\alpha}\gamma_p\sum_{m=1}^{4}(-1)^m\left[\frac{1}{z^{1/2}}(\tfrac{1}{3}\bar{\zeta}_m^{3/2}+\zeta_m^{1/2}\zeta_m)\right.$$
$$\left.-2z^{1/2}\bar{\zeta}_m^{1/2}+(2z-\bar{\zeta}_m-\zeta_m)ln(z^{1/2}+\bar{\zeta}_m^{1/2})\right]. \quad (5)$$

and

$$\chi(z) = \chi_1^{c,ext}(z)+\chi_2^c(z), \quad (6)$$

where

$$\chi_1^{c,ext}(z) = -\tfrac{1}{2}D\,e^{2i\alpha}\gamma_p\sum_{m=1}^{4}(-1)^m[(z-\zeta_m)-(\bar{z}-\bar{\zeta}_m)]ln(z-\zeta_m)$$
$$-\frac{1}{2}D\,e^{-2i\alpha}\gamma_p\sum_{m=1}^{4}(-1)^m[(z-\bar{\zeta}_m)-(\bar{z}-\zeta_m)]ln(z-\bar{\zeta}_m), \quad (7)$$

$$\chi_2^c(z) = -(z-\bar{z})\Phi_2^{c\prime}(z). \quad (8)$$

In equations (4), (5) and (7), α is the constant angle of slip in the regions R and $\bar{\mathrm{R}}$, $\zeta_m = \xi_m + i\eta_m$ $(m = 1,\ldots,4)$ are the locations of the corners of the active element, and $D = \mu/[2\pi(1-\nu)]$ where μ is the shear modulus and ν is Poisson's ratio. The superposed bar denotes the complex conjugate of a quantity and in equation (8), the prime denotes differentiation with respect to z. For the case where the point z lies within the region R, the complex potential functions are

$$\Phi(z) = \Phi_1^{c,inf}(z)+\Phi_2^c(z), \quad (9)$$

where

$$\Phi_1^{c,inf}(z) = \Phi_1^{c,ext}(z)+i\frac{\pi}{2}D\gamma_p(z)(1+e^{2i\alpha}), \quad (10)$$

and

$$\chi(z) = \chi_1^{c,inf}(z)+\chi_2^c(z), \quad (11)$$

where

$$\chi_1^{c,inf}(z) = \chi_1^{c,ext}(z)-\pi D\gamma_p(z)\sin 2\alpha. \quad (12)$$

The stress components are related to the complex potential functions through the equations

$$\tfrac{1}{2}(\sigma_{11}+\sigma_{22}) = 2\,\mathrm{Re}\,\Phi(z), \quad (13)$$

$$\tfrac{1}{2}(\sigma_{22}-\sigma_{11})+i\sigma_{12} = \chi(z), \quad (14)$$

where Re denotes the real part of a complex function. Details of the derivation of the complex potential functions for the planar slip element are given in the work of Denda (1983a).

THE FRACTURE PROCESS ZONE

The continuum model for a growing plane strain tensile crack in an elastic-ideally plastic solid predicts a logarithmic plastic strain singularity at the crack tip (Rice, 1968). Integration of the strain–displacement relations leads to a vanishing crack opening displacement and an infinite crack surface slope at the crack tip. The nonblunted appearance of the crack tip is a consequence of the inability of continuum plasticity theory to account for the material failure at the tip of the advancing crack. The material failure can be described by introducing a fracture process zone model in the region immediately ahead of the crack tip.

Weertman (1978) has suggested that in ductile materials under plane strain conditions, the nucleation of microvoids ahead of the crack tip can lead to localized necking of the material. Crack growth occurs when microvoids coalesce and join together with the existing crack. Detailed studies of this mechanism during fracture initiation and the early stages of crack growth have been provided by Aravas and McMeeking (1985) and Needleman and Tvergaard (1987). The central feature of these studies is the use of large deformation finite element analysis in conjunction with modified constitutive relations for the void-permeated material ahead of the crack tip. Both investigations give detailed estimates of the crack tip opening displacement required for fracture initiation. The latter study (Needleman and Tvergaard, 1987) also gives an estimate of the tearing modulus associated with the initial period of crack growth.

Rice and Sorenson (1978) have discussed the differences between the near-tip plastic strain fields which characterize stationary and extending cracks in elastic ideally plastic material. They note that the stationary crack is characterized by a strong $1/r$ type plastic strain singularity and that the extending crack is characterized by a much weaker $\ln(r)$ type plastic strain singularity (r is the distance from the crack tip). In addition, they present a general expression for the crack opening displacement which applies for both cases. For the stationary crack, this expression contains a parameter which can be accurately calculated only through a finite strain analysis. For the extending crack under constant load (which corresponds to the steady crack growth problem considered in this study), the expression reduces to a simplified form which allows for the crack opening displacement to be estimated from the results of conventional infinitesimal deformation analyses. This suggests that the effect of finite strain in the steady crack growth problem is confined to a very small region close to the crack tip. For this reason, it seems plausible that a simplified fracture process zone model can be used to quantify the fracture criterion for steady ductile crack growth.

The simplified fracture process zone model for steady crack growth must provide good estimates of the crack tip opening displacement and the length of the fracture process zone along the prolongation plane ahead of the crack tip. These quantities can then be used to calculate the critical crack tip opening angle associated with steady crack growth. Approximate models for the fracture process zone ahead of an extending crack have been used in previous work. Wnuk (1974) has employed the strip-yielding model of Bilby *et al.* (1963) and Dugdale (1960) (hereafter referred to as the BCS–Dugdale model) to formulate his final stretch criterion for plane stress crack growth. In Wnuk's model, yielding is confined to the crack prolongation line, and it is assumed that the condition for continued crack growth is the attainment of a critical increment of crack opening in a small segment of the yielded zone ahead of the crack tip. These quantities define a critical crack tip opening angle for continued crack growth. Rice and Sorenson (1978) have noted the similarity between Wnuk's final stretch concept and their own critical crack tip opening angle for continued plane strain crack growth. In an analytical study of fatigue crack growth, Budiansky and Hutchinson (1978) have employed a modified version of the BCS–Dugdale model that accounts for cyclic loading and the residually stretched material appended to the crack surfaces. This model successfuly predicts the fatigue crack closure phenomenon discovered by Elber (1970) in an experimental study of fatigue crack growth. The Budiansky and Hutchinson study indicates that fatigue crack closure occurs when material that is plastically stretched in the strip-yielding zone falls behind the advancing crack tip and comes into contact during the cyclic loading.

The previous investigations of Wnuk (1974) and Budiansky and Hutchinson (1978) establish the usefulness of the BCS–Dugdale model for the representation of ductile material failure ahead of the crack tip. For this reason, the BCS–Dugdale model will be employed in this study to represent the fracture process zone associated with a steadily propagating plane strain tensile crack under constant loading. The fracture process zone ahead of the advancing tensile crack is modeled as a continuous distribution of edge dislocations with Burgers vectors parallel to the x_2-axis. The complex potential functions for an edge dislocation with Burgers vector b located at $x_1 = x'$ are

$$\phi_s'(z) = \frac{\mu b}{4\pi(1-\nu)}\frac{1}{z-x'} - \frac{\mu b}{4\pi(1-\nu)}\frac{1}{z^{1/2}(z^{1/2}+x'^{1/2})}, \tag{15}$$

$$\bar{\Omega}_s'(\bar{z}) = \frac{\mu b}{4\pi(1-\nu)}\frac{1}{\bar{z}-x'} - \frac{\mu b}{4\pi(1-\nu)}\frac{1}{\bar{z}^{1/2}(\bar{z}^{1/2}+x'^{1/2})}, \tag{16}$$

where the first term in the foregoing equations represents the self-stresses of the dislocation and the second term represents the image stresses resulting from the condition of zero normal traction along the crack surface. The stress components are related to the complex potential functions through the equations

$$\tfrac{1}{2}(\sigma_{11}+\sigma_{22}) = 2\ \mathrm{Re}\ \phi_s'(z), \tag{17}$$

$$\tfrac{1}{2}(\sigma_{22}-\sigma_{11})-\mathrm{i}\sigma_{12} = \bar{\Omega}_s'(\bar{z})-\bar{\phi}_s'(\bar{z})+(z-\bar{z})\bar{\phi}_s''(\bar{z}) = (z-\bar{z})\bar{\phi}_s''(\bar{z}). \tag{18}$$

THE ELASTIC SINGULAR FIELD DUE TO EXTERNAL LOADING

The remote tensile stress acting on the infinite body containing the steadily propagating crack gives rise to the mode I singular stress field of linear elastic fracture mechanics in the region near the crack tip. The complex potential functions for the elastic singular field are

$$\phi_{rem}'(z) = \frac{K}{2(2\pi z)^{1/2}}, \tag{19}$$

$$\bar{\Omega}_{rem}'(\bar{z}) = \frac{K}{2(2\pi\bar{z})^{1/2}}, \tag{20}$$

where K is the mode I stress intensity factor. The stress components for the elastic singular field can be obtained by using the complex potential function of eqns (19) and (20) in eqns (17) and (18). Introducing polar coordinates through the relation $z = r\,\mathrm{e}^{\mathrm{i}\theta}$, the stresses can be expressed in the form

$$\sigma_{11} = \frac{K}{(2\pi r)^{1/2}} f_{11}(\theta) = \frac{K}{(2\pi r)^{1/2}} \cos\frac{\theta}{2}\left(1-\sin\frac{\theta}{2}\sin\frac{3\theta}{2}\right), \tag{21}$$

$$\sigma_{22} = \frac{K}{(2\pi r)^{1/2}} f_{22}(\theta) = \frac{K}{(2\pi r)^{1/2}} \cos\frac{\theta}{2}\left(1+\sin\frac{\theta}{2}\sin\frac{3\theta}{2}\right), \tag{22}$$

$$\sigma_{12} = \frac{K}{(2\pi r)^{1/2}} f_{12}(\theta) = \frac{K}{(2\pi r)^{1/2}} \sin\frac{\theta}{2}\cos\frac{\theta}{2}\cos\frac{3\theta}{2}. \tag{23}$$

SUPERPOSITION OF RESULTS AND APPLICATION OF THE YIELD CONDITION

The stress components due to inelastic deformation in the planar slip element and fracture process zone and the elastic singular stresses due to the remote tensile loading have been obtained from complex potential functions appropriate for two-dimensional problems in the theory of elasticity. Plastic deformation in a cracked body can be considered as an interaction between the deformation field of dislocation arrays and the elastic field associated with the applied loading. The stresses, strains and displacements for the planar slip element, the fracture process zone, and the elastic applied loading field can be superposed to model the plastic deformation near a steadily growing plane strain tensile crack. Unknown quantities associated with the planar slip elements and fracture process zone, as well as the extent of the region of plastic deformation, can then be found through the application of a yield condition.

Consider the region surrounding the crack in the upper half-plane $x_2 > 0$ to be divided into N rectangular elements. Each element represents the active portion of the region R shown in Fig. 2. By superposing the stresses due to (i) inelastic deformation in the N regions $R + \bar{R}$ associated with each rectangular element, (ii) the continuous distribution of dislocations in the fracture process zone, and (iii) the elastic singular field of the applied loading, the stresses at all points in the plastically deforming body can be obtained. Let τ_0 be the yield stress in shear for an ideally plastic material. Introducing the dimensionless variables

$$\hat{z} = \frac{\tau_0^2}{K^2} z, \qquad \hat{\zeta} = \frac{\tau_0^2}{K^2} \zeta, \qquad \hat{\gamma}_p = \frac{\mu}{\tau_0} \gamma_p, \qquad \tau = \frac{\tau_0^2}{K^2} a, \qquad \hat{\sigma}_{\alpha\beta} = \frac{\sigma_{\alpha\beta}}{\tau_0}, \qquad \hat{h} = \frac{\mu}{\tau_0} h, \tag{24}$$

where the indices $\alpha, \beta = 1, 2$, the stresses at any point $\hat{z} = \hat{x}_1 + i\hat{x}_2$ can be expressed as

$$\hat{\sigma}_{\alpha\beta}(\hat{z}) = \sum_{j=1}^{N} \hat{\sigma}^p_{\alpha\beta}(\hat{z}, \hat{\zeta}_j) + \hat{\sigma}^c_{\alpha\beta}(\hat{z}) + \hat{\sigma}^e_{\alpha\beta}(\hat{z}), \tag{25}$$

where $\hat{\sigma}^p_{\alpha\beta}(\hat{z}, \hat{\zeta}_j)$ is the stress due to the inelastic deformation in the jth planar slip element with center at $\hat{\zeta}_j = \hat{\xi}_j + i\hat{\eta}_j$, $\hat{\sigma}^c_{\alpha\beta}(\hat{z})$ is the stress due to the continuous distribution of dislocations in the fracture process zone, and $\sigma^e_{\alpha\beta}(\hat{z})$ is the stress due to the elastic singular field of the applied loading. Using eqns (3) (14), the stresses from the planar slip element can be expressed as

$$\tfrac{1}{2}[\hat{\sigma}^p_{22}(\hat{z}, \hat{\zeta}_j) - \hat{\sigma}^p_{11}(\hat{z}, \hat{\zeta}_j)] = \frac{1}{2\pi(1-\nu)} [\hat{A}(\hat{z}, \hat{\zeta}_j) \cos 2\alpha_j + \hat{B}(\hat{z}, \hat{\zeta}_j) \sin 2\alpha_j]_{\hat{\gamma}_p}^{\hat{\gamma}_j}, \tag{26}$$

$$\hat{\sigma}^p_{12}(\hat{z}, \hat{\zeta}_j) = \frac{1}{2\pi(1-\nu)} [\hat{C}(\hat{z}, \hat{\zeta}_j) \cos 2\alpha_j + \hat{D}(\hat{z}, \hat{\zeta}_j) \sin 2\alpha_j]_{\hat{\gamma}_p}^{\hat{\gamma}_j}, \tag{27}$$

$$\tfrac{1}{2}[\hat{\sigma}^p_{22}(\hat{z}, \hat{\zeta}_j) + \hat{\sigma}^p_{11}(\hat{z}, \hat{\zeta}_j)] = \frac{1}{2\pi(1-\nu)} [\hat{P}(\hat{z}, \hat{\zeta}_j) \cos 2\alpha_j + \hat{Q}(\hat{z}, \hat{\zeta}_j) \sin 2\alpha_j]_{\hat{\gamma}_p}^{\hat{\gamma}_j}, \tag{28}$$

where α_j is the angle of slip in the jth element and the dot now denotes differentiation with respect to the dimensionless time τ. The functions $\hat{A}$, $\hat{B}$, $\hat{C}$, $\hat{D}$, $\hat{P}$, $\hat{Q}$ are given in polar coordinate form in the work of Denda (1983b). The stresses due to the continuous distributions in the fracture process zone are given by

$$\tfrac{1}{2}[\hat{\sigma}^c_{22}(\hat{z}) - \hat{\sigma}^c_{11}(\hat{z})] = \frac{1}{2\pi(1-\nu)} \int_0^{\hat{c}} \hat{b}(\hat{x}') \hat{H}_2(\hat{z}, \hat{x}')\, d\hat{x}', \tag{29}$$

$$\hat{\sigma}^c_{12}(\hat{z}) = \frac{1}{2\pi(1-\nu)} \int_0^{\hat{c}} \hat{b}(\hat{x}') \hat{H}_3(\hat{z}, \hat{x}')\, d\hat{x}', \tag{30}$$

$$\tfrac{1}{2}[\hat{\sigma}^{\infty}_{22}(\hat{z})+\hat{\sigma}^{\infty}_{11}(\hat{z})] = \frac{1}{2\pi(1-\nu)}\int_0^{\hat{x}^*} \hat{b}(\hat{x}')\hat{H}_1(\hat{z},\hat{x}')\,\mathrm{d}\hat{x}', \tag{31}$$

where $\hat{b}(\hat{x})$ is the dislocation density, and $\hat{x}^*$ is the extent of the fracture process zone along the positive $\hat{x}_1$-axis. The functions $\hat{H}_1$, $\hat{H}_2$, $\hat{H}_3$ are obtained from eqns (15)–(18). They are given in polar coordinate form in the thesis of the author (Russell, 1987). Finally, the stresses due to the applied loading are given in eqns (21)–(23), which can be expressed in dimensionless form using eqn (24).

The yield condition used in the solution consists of two requirements: (i) the maximum shear stress at the centerpoint z_k of the kth active element is equal to the yield stress in shear, τ_0, and (ii) the direction of the maximum shear stress in the kth active element must coincide with the direction α_k of the maximum plastic shear strain rate. These requirements can be expressed in terms of the dimensionless variables by the two equations

$$\tfrac{1}{2}[\hat{\sigma}_{22}(\hat{z}_k)-\hat{\sigma}_{11}(\hat{z}_k)]\sin 2\alpha_k+\hat{\sigma}_{12}(\hat{z}_k)\cos 2\alpha_k = 1, \tag{32}$$

$$\tfrac{1}{2}[\hat{\sigma}_{22}(\hat{z}_k)-\hat{\sigma}_{11}(\hat{z}_k)]\cos 2\alpha_k-\hat{\sigma}_{12}(\hat{z}_k)\sin 2\alpha_k = 0. \tag{33}$$

Denda (1983a) gives an equivalent form which is more convenient for computational purposes:

$$\tfrac{1}{2}[\hat{\sigma}_{22}(\hat{z}_k)-\hat{\sigma}_{11}(\hat{z}_k)] = \sin 2\alpha_k. \tag{34}$$

$$\hat{\sigma}_{12}(\hat{z}_k) = \cos 2\alpha_k. \tag{35}$$

The requirement of the yield condition for coincident directions of maximum shear stress and maximum plastic shear rate implies that the material is elastically incompressible with Poisson's ratio $\nu = 1/2$. This can be seen by employing dimensioned variables, squaring both sides of eqns (34) and (35), and adding the result to obtain

$$\tfrac{1}{4}(\sigma_{22}-\sigma_{11})^2+\sigma_{12}^2 = \tau_0^2. \tag{36}$$

Equation (36) is von Mises' yield condition for an elastically incompressible, ideally plastic material.

The solution for the unknown dislocation density in the fracture process zone is obtained by prescribing the normal stress $\hat{\sigma}_{nn}$ along the $\hat{x}_1$-axis ahead of the crack tip. For this purpose it is appropriate to employ the result $\hat{\sigma}_{nn} = 5.106$, obtained from the asymptotic analysis of the mode I plane strain growing crack given by Drugan *et al.* (1982). The prescribed stress requirement is consistent with the assumption that steady crack growth is deformation-controlled and characterized by a constant critical value of the crack tip opening angle. As noted by Rice *et al.* (1980), the critical crack tip opening angle criterion makes no reference to the normal stress ahead of the crack tip, which is essentially equal to the Prandtl field value for both stationary and growing cracks. Instead, it reflects the fact that the strain and crack opening displacement are the only variable features of the near-tip fields associated with plane strain cracks in elastic–plastic materials.

NUMERICAL SOLUTION PROCEDURE

A system of nonlinear equations governing the steady state tensile crack growth problem can be obtained by substituting the stresses from eqn (25) into eqns (34) and (35) and employing the prescribed value $\hat{\sigma}_{22} = \hat{\sigma}_{nn}$ in the fracture process zone. This procedure gives a system of $2N+1$ nonlinear equations that can be solved for the unknown quantities $\hat{\gamma}^{p}_{0}$, α_j $(j = 1, \ldots, N)$ associated with the planar slip elements and the dislocation density $\hat{b}(\hat{x})$ in the fracture process zone. The application of numerical methods to the solution of

this system of equations requires discretization of the integrals involving the dislocation density. For this purpose, the integration domain is divided into $3n$ equal intervals of length

$$\Delta\hat{x} = \frac{\hat{x}^*}{3n}. \tag{37}$$

Mesh points are then placed at the center of each interval, giving

$$\hat{x}_j = \tfrac{1}{2}\Delta\hat{x} + (j-1)\Delta\hat{x} \qquad \text{for } j = 1, \ldots, 3n. \tag{38}$$

An integration formula can then be obtained for each integral by representing the integrand by a Lagrange interpolating polynomial of degree two and integrating the result over a subdomain of three intervals. The definition of the Cauchy principal value integral is employed for the case where the integrand possesses a singularity of Cauchy's type. The integrals involved in the yield condition can then be expressed as

$$\tfrac{1}{2}[\hat{\sigma}_{22}(\hat{x}_k) - \hat{\sigma}_{11}(\hat{x}_k)] = \frac{1}{2\pi(1-\nu)} \int_0^{\hat{x}^*} \hat{b}(\hat{x}')\hat{H}_2(\hat{x}_k, \hat{x}')\, \mathrm{d}\hat{x}' \approx \sum_{j=1}^{3n} \hat{b}_j I_{k,j}^{(1)} \tag{39}$$

for $k = 1, \ldots, N$,

$$\hat{\sigma}_{12}(\hat{x}_k) = \frac{1}{2\pi(1-\nu)} \int_0^{\hat{x}^*} \hat{b}(\hat{x}')\hat{H}_3(\hat{x}_k, \hat{x}')\, \mathrm{d}\hat{x}' \approx \sum_{j=1}^{3n} \hat{b}_j I_{k,j}^{(2)} \tag{40}$$

for $k = 1, \ldots, N$,

$$\begin{aligned} \hat{\sigma}_{22}(\hat{x}_k) &= \frac{1}{2\pi(1-\nu)} \int_0^{\hat{x}^*} \hat{b}(\hat{x}')[\hat{H}_1(\hat{x}_k, \hat{x}') + \hat{H}_2(\hat{x}_k, \hat{x}')]\, \mathrm{d}\hat{x}' \\ &= \frac{1}{2\pi(1-\nu)} \int_0^{\hat{x}^*} b(\hat{x}') \left[\frac{1}{\hat{x}_k - \hat{x}'} - \frac{1}{\hat{x}_k^{1/2}(\hat{x}_k^{1/2} + \hat{x}'^{1/2})} \right] \mathrm{d}\hat{x}' \approx \sum_{j=1}^{3n} \hat{b}_j I_{k,j}^{(3)} \end{aligned} \tag{41}$$

for $k = 1, \ldots, 3n$ where the notation $\hat{b}(\hat{x}_j') = \hat{b}_j$ has been employed. Detailed expressions for the quantities $I_{k,j}^{(1)}$, $I_{k,j}^{(2)}$, $I_{k,j}^{(3)}$, are given in the thesis of the author (Russell, 1987).

The use of eqns (39)–(41) enables us to write $2N+3n$ nonlinear algebraic equations for the unknown quantities $\hat{\gamma}_p^j$, α_j $(j = 1, \ldots, N)$ and $\hat{b}_j$ $(j = 1, \ldots, 3n)$. The nonlinearity can be expressed in a weaker form by making the substitutions

$$\hat{w}_{1j} = \hat{\gamma}_p^j \cos 2\alpha_j, \tag{42}$$

$$\hat{w}_{2j} = \hat{\gamma}_p^j \sin 2\alpha_j, \tag{43}$$

for $j = 1, \ldots, N$. The resulting system of equations takes the form

$$\begin{aligned} \frac{1}{2\pi(1-\nu)} \sum_{\substack{j=1 \\ j \neq k}}^{N} \hat{C}(\hat{\xi}_k, \hat{\xi}_j)\hat{w}_{1j} + \left[\frac{1}{2\pi(1-\nu)} \hat{C}(\hat{\xi}_k, \hat{\xi}_k) - \frac{1}{\hat{\gamma}_p^k} \right] \hat{w}_{1k} + \frac{1}{2\pi(1-\nu)} \sum_{j=1}^{N} \hat{D}(\hat{\xi}_k, \hat{\xi}_j)\hat{w}_{2j} \\ + \sum_{j=1}^{3n} \hat{b}_j I_{k,j}^{(2)} = -\frac{1}{(2\pi\hat{r}_k)^{1/2}} f_{12}(\theta_k) \end{aligned} \tag{44}$$

for $k = 1, \ldots, N$,

$$\frac{1}{2\pi(1-\nu)}\sum_{j=1}^{N}\hat{A}(\hat{\xi}_k,\hat{\zeta}_j)\hat{w}_{1j}+\frac{1}{2\pi(1-\nu)}\sum_{\substack{j=1\\ j\neq k}}^{N}\hat{B}(\hat{\xi}_k,\hat{\zeta}_j)\hat{w}_{2j}+\left[\frac{1}{2\pi(1-\nu)}\hat{B}(\hat{\xi}_k,\hat{\zeta}_k)-\frac{1}{\hat{\gamma}_p^{k}}\right]\hat{w}_{2k}$$
$$+\sum_{j=1}^{3n}\hat{b}_j I_{k,j}^{(1)} = -\frac{1}{2(2\pi\hat{r}_k)^{1/2}}[f_{22}(\theta_k)-f_{11}(\theta_k)] \quad (45)$$

for $k = 1, \ldots, N$ and

$$\frac{1}{2\pi(1-\nu)}\sum_{j=1}^{N}[\hat{A}(\hat{x}_k,\hat{\zeta}_j)+\hat{P}(\hat{x}_k,\hat{\zeta}_j)]\hat{w}_{1j}+\frac{1}{2\pi(1-\nu)}\sum_{j=1}^{N}[\hat{B}(\hat{x}_k,\hat{\zeta}_j)+\hat{Q}(\hat{x}_k,\hat{\zeta}_j)]\hat{w}_{2j}$$
$$+\sum_{j=1}^{3n}\hat{b}_j I_{k,j}^{(3)} = \hat{\sigma}_{nn}-\frac{1}{(2\pi\hat{x}_k)^{1/2}} \quad (46)$$

for $k = 1, \ldots, 3n$. It is noted that the nonlinearity in eqns (44) and (45) is confined to one term and that eqn (46) represents a set of linear algebraic equations.

The system of eqns (44)–(46) is solved by an iterative scheme. In the first iteration, the quantities $f_k^* = 1/\hat{\gamma}_p^{k}$ are set equal to zero. After solving the resulting system of linear algebraic equations, the quantities $\hat{\gamma}_p^{k}$ and f_k^* can be calculated from the relations

$$\hat{\gamma}_p^{k} = (\hat{w}_{1k}^2+\hat{w}_{2k}^2)^{1/2}, \quad (47)$$

$$f_k^* = 1/\hat{\gamma}_p^{k}, \quad (48)$$

for $k = 1, \ldots, N$. The positive root is taken in eqn (47) since the requirement of positive plastic work rate in each element implies that $\hat{\gamma}_p^{k} > 0$. The quantities f_k^* are now inserted into eqns (44) and (45) and the solution process continues. The iterations proceed until the quantities $|f_k^{*(i)}-f_k^{*(i-1)}|/f_k^{*(i)}$ computed from iterations i and $i-1$ are sufficiently small. When a convergent solution to the system of eqns (44)–(46) has been obtained, the angles α_k ($k = 1, \ldots, N$) of the maximum plastic shear strain rate can be calculated by using eqns (42) and (43) in conjunction with the physical requirement that $0 \leqslant \alpha_k \leqslant \pi$ for each plastically deforming element in the upper half-plane $\hat{x}_2 > 0$.

The extent of the region of active plastic deformation in the upper half-plane $\hat{x}_2 > 0$ and the length $\hat{x}^*$ of the fracture process zone along the positive $\hat{x}_1$-axis are unknown at the beginning of the calculations. The extent of the active plastic zone in the upper half-plane is determined by covering a large portion of the crack tip region with a rectangular mesh of elements and then activating N of these elements based upon an estimate of the size and shape of this zone. After a solution to the system of eqns (44)–(46) has been obtained, stresses are calculated at the center of each element in the mesh. Inactive elements which do not satisfy the condition

$$\tfrac{1}{4}[\hat{\sigma}_{22}(\hat{\xi}_k)-\hat{\sigma}_{11}(\hat{\xi}_k)]^2+\hat{\sigma}_{12}^2(\hat{\xi}_k) \leqslant 1 \quad (49)$$

are considered to be active elements in the next round of calculations. Active elements which hinder the convergence of the solution of the system of eqns (44)–(46) by virtue of extremely small plastic shear strain rates $\hat{\gamma}_p^{k}$ are considered to be inactive in the next round of calculations. Usually two or three rounds of calculation are sufficient to determine the active plastic zone corresponding to a given fracture process zone length $\hat{x}^*$.

The length of the fracture process zone $\hat{x}^*$ is determined from the condition that the stress singularity associated with the elastic applied loading field be cancelled by the plastic deformation in the planar slip elements and fracture process zone. Denda (1983a) has shown that all of the stress components due to the inelastic deformation in the planar slip

element possess a term containing the inverse square root singularity that characterizes the elastic field of the applied loading. From each of these terms a common factor can be extracted which gives a measure of the elastic singularity cancellation associated with the planar slip element. Physically, these singularity-cancelling parameters are associated with the dislocation image stress field of each element. A similar singularity-cancelling parameter can be extracted from the image stress field associated with the continuous distribution of edge dislocations in the fracture process zone. Adding the singularity-cancelling parameters from the N planar slip elements and fracture process zone with the associated parameter from the elastic singular field gives the quantity

$$\Delta\hat{e} = \frac{1}{2(2\pi)^{1/2}} - \frac{1}{2\pi(1-\nu)} \sum_{j=1}^{N} \frac{\hat{s}_j}{\hat{r}_p} \sum_{m=1}^{4} \{(-1)^m \tfrac{4}{3} \hat{s}_m'^{1/2} [\cos^3(\phi_m'/2)\cos 2\alpha_j + \sin^3(\phi_m'/2)\sin 2\alpha_j]\}$$

$$- \frac{1}{4\pi(1-\nu)} \sum_{k=1}^{n} \tfrac{1}{8}\Delta\hat{x} \left[9\hat{b}_{3k-2} \frac{1}{\hat{x}_{3k-2}^{1/2}} + 6\hat{b}_{3k-1} \frac{1}{\hat{x}_{3k-1}^{1/2}} + 9\hat{b}_{3k} \frac{1}{\hat{x}_{3k}^{1/2}} \right]. \quad (50)$$

where $\hat{s}_m'$, ϕ_m' $(m = 1, \ldots, 4)$ are the polar coordinates of the four corners of the active portion of planar slip element j. The final summation in eqn (50) is obtained by using the numerical integration scheme employed previously to discretize integrals involving the dislocation density. It is convenient to normalize $\Delta\hat{e}$ by defining $\Delta\hat{e}^* = 2(2\pi)^{1/2}\Delta\hat{e}$. The size of the fracture process zone $\hat{x}^*$ corresponding to a given mesh of planar slip elements is adjusted until $\Delta\hat{e}^* \approx 0$.

The crack tip opening displacement, δ_0, associated with the fracture process zone ahead of the propagating crack tip is obtained through the relation

$$\delta_0 = \int_0^{x^*} h(x')\,dx'. \quad (51)$$

Introducing the dimensionless variable $\hat{\delta}_0 = \delta_0/[K^2/\mu\tau_0]$ and the numerical integration scheme discussed previously yields the formula

$$\hat{\delta}_0 = \sum_{k=1}^{n} \tfrac{1}{8}\Delta\hat{x}(9\hat{b}_{3k-2} + 6\hat{b}_{3k-1} + 9\hat{b}_{3k}) \quad (52)$$

for numerical evaluation of the crack tip opening displacement.

NUMERICAL RESULTS

The numerical solution procedure described in the previous section has been implemented to study the influence of the fracture process zone on the steady state, plane strain tensile crack growth problem. The region of active plastic deformation near the advancing crack tip was determined by using a series of increasingly refined planar slip element meshes to identify the region in the upper half-plane where the yield condition is satisfied. The length of the fracture process zone was determined through the requirement that the stress singularity associated with the elastic applied loading field must be cancelled by the plastic deformation in the planar slip elements and fracture process zone. For this purpose, the two elements nearest the crack tip were subdivided several times in order to simulate the intense yielding that occurs in this region.

The solution corresponding to the finest element mesh employed in the calculation is shown in Fig. 3. The planar slip element mesh consists of only 106 elements, as compared to the 1660 elements used in Sorenson's (1979) finite element analysis of plane strain tensile crack growth. As noted by Denda (1983b), the planar slip element method requires a less elaborate element mesh because the influence of the active elements on the stresses, strains, and displacements is calculated directly through the use of potential functions. In contrast,

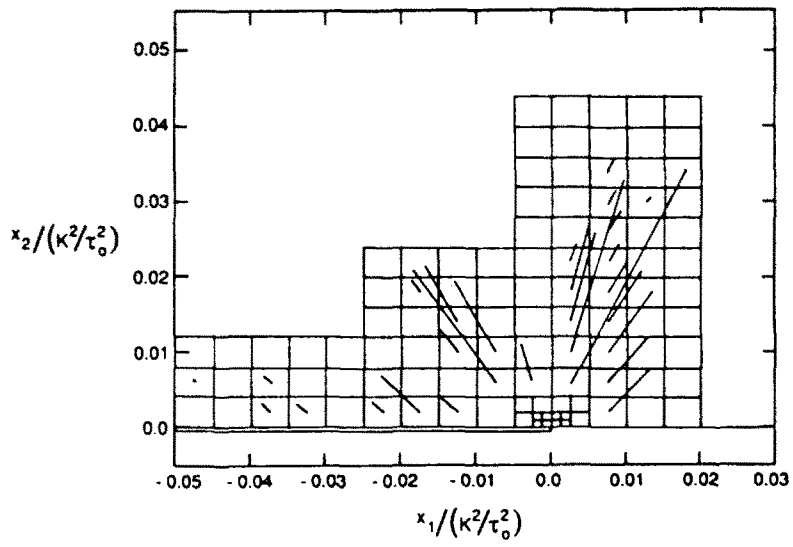

Fig. 3. Mesh and numerical solution for the planar slip elements when the fracture process zone is included in the model.

the finite element method requires a much larger mesh because the influence of remote elements on the deformation at a given point must be propagated through intermediate elements. These intermediate elements must be highly refined to prevent loss of numerical accuracy. For this reason it is expected that the planar slip element method gives results that are competitive in accuracy with finite element method results obtained on much more detailed meshes.

In the 106 element mesh shown in Fig. 3, 40 elements were determined to satisfy the yield condition. Thirty-three mesh points were employed in the fracture process zone, giving a total of 113 equations in 113 unknowns to be solved during each iteration. Fifty iterations were sufficient to obtain accurate solution to the system of eqns (44)–(46). The magnitude of the plastic shear strain rate $\dot{\gamma}_p^{\alpha}$ and the direction of slip α are represented as scaled line segments emanating from the centers of the active elements of the mesh. The solution of the elements near the crack tip is not shown due to the large magnitude of the plastic shear strain rate in this region.

Figure 3 reveals four distinct sectors of deformation in the region near the advancing crack tip. In terms of the polar angle θ measured from the positive $\hat{x}_1$-axis, they are

(i) a plastically deforming sector located in the region $0 \leqslant \theta \leqslant 45^\circ$ where the slip angle is nearly constant at $\alpha \approx 45^\circ$,

(ii) a plastically deforming centered-fan sector located in the region $45^\circ \leqslant \theta \leqslant 135^\circ$ where the slip angle $\alpha \approx \theta$ for elements near the crack tip,

(iii) an elastically deforming sector located in the region $135^\circ \leqslant \theta \leqslant 161^\circ$,

(iv) a secondary plastically deforming sector located in the region $161^\circ \leqslant \theta \leqslant 180^\circ$ in which the slip angle is nearly constant at $\alpha \approx 135^\circ$.

The length of the fracture process zone corresponding to 97.3% singularity cancellation was determined to be $\hat{x}^* = 0.0007$, which is less than the horizontal extent of the smallest element adjacent to the crack tip. Note that the spatial coordinates in Fig. 3 have been normalized by the quantity K^2/τ_0^2, where τ_0 is the yield stress in shear. In finite element studies the spatial coordinates are often normalized by K^2/σ_0^2, where σ_0 is the yield stress in uniaxial tension. Comparisons between different sets of results can be obtained by taking $\sigma_0 = (3)^{1/2}\tau_0$.

The solution for the same element mesh in the absence of the fracture process zone is shown in Fig. 4. In contrast to the results shown in Fig. 3, only 75.5% singularity cancellation is obtained by the planar slip elements acting alone. The configuration of active

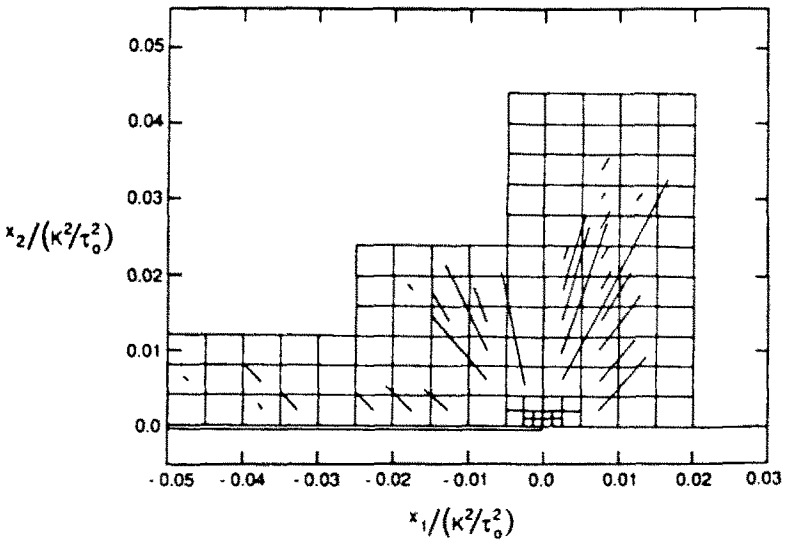

Fig. 4. Mesh and numerical solution for the planar slip elements when the fracture process zone is omitted from the model.

elements and the features of the solution for the elements outside the near-tip region are similar for the two cases. The global elastic plastic solution of Fig. 4 also agrees closely with the planar slip element results obtained by Denda (1983a). The influence of the fracture process zone is apparent from an examination of the solution in the near-tip elements not shown in Figs 3 and 4. For this purpose, numerical results for the near-tip elements are given in Table 1. The quantities $\frac{s}{\tau_0}^{(1)}$, $\chi^{(1)}$ refer to the slip element solutions when the fracture process zone is included and the quantities $\frac{s}{\tau_0}^{(2)}$, $\chi^{(2)}$ refer to the slip element solutions when the fracture process zone is omitted. The quantity θ is the polar angle at the center of the element and χ_a is the slip angle predicted at the center of the element by the asymptotic analysis of Drugan *et al.* (1982). Elements with centerpoints lying in the elastically deforming sector are indicated by a blank in the appropriate slip angle entry in the table. A diagram showing the location of the numbered elements is given in Fig. 5.

Table 1. Numerical results for near-tip elements

Element	θ (degrees)	$\frac{s}{\tau_0}^{(1)}$	$\frac{s}{\tau_0}^{(2)}$	$\chi^{(1)}$ (degrees)	$\chi^{(2)}$ (degrees)	χ_a (degrees)
1	165.4	0	0	—	—	135.0
2	165.1	0	0	—	—	135.0
3	166.5	0	0	—	—	135.0
4	144.2	4008.0	5327.3	110.06	96.64	—
5	38.66	3961.0	2414.5	57.58	49.40	45.0
6	14.93	1037.0	860.2	49.50	48.52	45.0
7	15.64	401.1	499.7	49.94	50.45	45.0
8	14.93	165.3	188.7	46.05	46.99	45.0
9	142.3	2372.6	2211.8	120.5	126.5	—
10	113.3	40.9	1597.5	104.6	86.9	—
11	66.68	3067.6	2469.5	71.0	65.4	66.68
12	37.72	1180.8	764.8	54.96	54.74	45.0
13	141.8	678.2	584.9	127.0	133.2	—
14	113.0	397.8	946.0	113.2	100.3	—
15	67.04	1677.3	1511.3	63.52	62.27	67.04
16	38.19	247.1	254.5	52.11	54.52	45.0
17	141.6	372.3	235.3	126.2	130.2	—
18	112.8	131.2	296.9	108.2	102.5	—
19	67.21	645.1	607.9	61.60	62.48	67.21
20	38.43	160.2	146.3	48.85	50.56	45.0

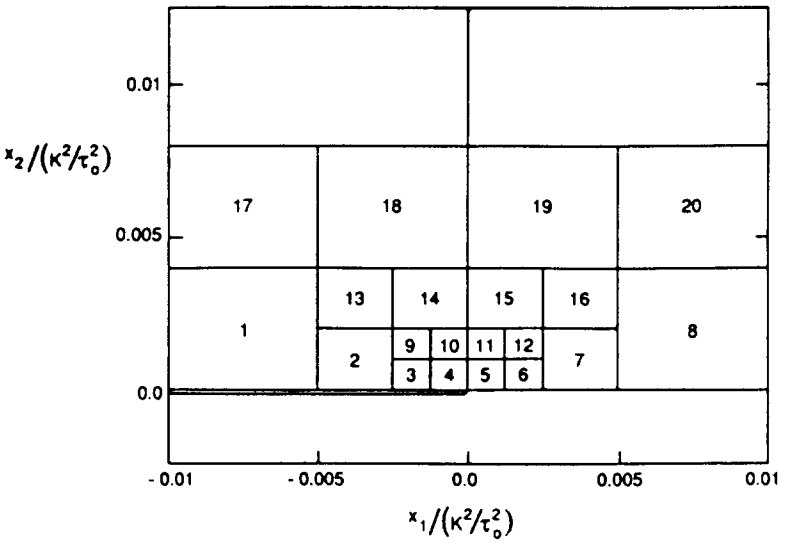

Fig. 5. Diagram of near-tip elements.

Examination of Table 1 reveals that the greatest differences in elemental strain rate magnitude for the two numerical solutions are found in elements 4, 5, 10, 11 and 14. Of these five elements, elements 4, 10 and 14 are also characterized by an appreciable discrepancy in the two numerically calculated slip angles. These differences arise from the incomplete elastic singularity cancellation associated with the planar slip elements acting alone. In the solution obtained with the fracture process zone, it is noted that the plastic shear strain rates $\dot{\gamma}_p^{(1)}$ in elements 10 and 14 are rather small, and that the slip angles $\alpha^{(1)}$ for these elements are 104.6° and 113.2°, respectively. These results, along with the result that $\alpha^{(1)} = 110.06°$ in element 4, suggest some curvature in the boundary between the centered-fan plastic sector and the elastic sector behind the crack tip. This boundary is located at $\theta = 135°$ for the far field elements shown in Fig. 3 and curves toward the $\theta = 110°$ direction for the elements very close to the crack tip. This curvature is consistent with the asymptotic analysis of Drugan *et al.* (1982), which predicts that the boundary between the centered-fan sector and the elastic sector is at $\theta = 112.1°$.

Denda (1983a) has found that as the near-tip element mesh is refined toward zero element size, the planar slip elements are capable of cancelling the entire elastic singularity associated with the applied loading. In this limit the results for the planar slip elements acting alone will converge toward the results of the asymptotic analysis based upon the infinitesimal deformation assumption. In particular, the crack tip will possess the zero crack tip opening displacement and infinite crack surface slope that are indicative of logarithmically singular plastic strains. In this same limit, the results for the planar slip element solution with the fracture process zone model will differ slightly from the asymptotic solution in the near-tip elements. A small fracture process zone will remain ahead of the crack tip, and a discrete value of the crack tip opening displacement will be obtained. When viewed in this way, the fracture process zone model is an approximate method of accounting for the presence of large but finite strains in the material ahead of the crack tip. The determination of the true fracture process zone size and crack tip opening angle associated with complete refinement of the elements adjacent to the crack tip is discussed in the next section.

The slip lines and elastic–plastic boundary constructed from the numerical solution that includes the fracture process zone are shown in Fig. 6. The plastic zone is composed of two lobe-shaped regions containing the primary plastic sectors (i) and (ii) discussed previously and a region along the crack surface containing the secondary plastic sector (iv) discussed previously. The plastic region ahead of the crack tip has its maximum extent

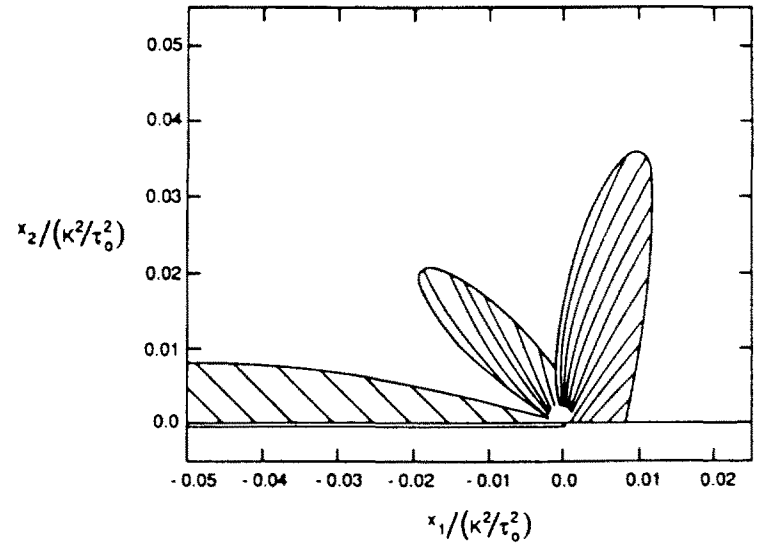

Fig. 6. Slip lines and elastic-plastic boundary when the fracture process zone is included in the model.

along the ray $\theta = 74^\circ$ and possesses centered-fan type slip lines that curve toward the positive $\hat{x}_1$ direction. The curvature of the slip lines in the plastic region ahead of the crack tip has been predicted by Rice (1968) in a discussion of the stationary tensile crack. The higher-order asymptotic analysis of Drugan (1986) predicts a similar type of curvature for the slip line that forms the border between the plastically deforming sectors (i) and (ii).

The lobe-shaped region of plastic deformation behind the crack tip has its maximum extent along the ray $\theta = 132^\circ$ and possesses centered-fan type slip lines that curve toward the $\hat{x}_2$ direction. This second lobe of plastic deformation is not present in finite element results for plane strain crack growth, e.g. Sorenson (1979) and Sham (1983), but it has been observed in previous work by Denda (1983a) using the dislocation-based planar slip element method. It has also been observed in recent work by Denda and Lua (1986), who studied steady state plane strain crack growth using a numerical method that is based upon the Green's function representation of inelastic deformation by a continuous distribution of force dipoles or couples. One possible reason for the discrepancy in the results obtained with the finite element method and those obtained with the Green's function methods is the procedures that are used to model crack growth. Most of the detailed finite element studies use a Lagrangian representation of crack growth. In this approach the coordinate system remains fixed and the crack propagates from node to node in the element mesh. In contrast, the Green's function methods (based upon either continuous distributions of dislocations or continuous distributions of force dipoles) use an Eulerian representation of crack growth. In the Eulerian approach, the coordinate system moves with the extending crack and time rates are calculated using the material derivative. The Lagrangian approach is suitable for studies of transient crack growth following fracture initiation, while the Eulerian approach is more appropriate for studies of steady crack growth. In this regard, a highly detailed Eulerian finite element study of steady crack growth would be useful for clarifying the differences between the finite element results and the planar slip element results in the plane strain crack growth problem. The methodology for such a work has been developed by Dean and Hutchinson (1980), and the results would be a valuable counterpart to Sham's (1983) detailed Lagrangian finite element results for transient plane strain crack growth.

Finally, Fig. 6 shows that a secondary plastic zone comprising the plastically deforming sector (iv) mentioned earlier extends along the surface of the crack. As noted by Drugan *et al.* (1982), the existence of this region is necessary because material elements passing through the centered-fan sector very close to the crack tip acquire very large plastic strains which necessitate further yielding to avoid unbounded residual stress. The calculations

presented here indicate that the yield condition is barely satisfied in the secondary plastic zone and that the plastic shear strain rate in the active planar slip elements of this region are rather small. For this reason, the secondary plastic zone has been terminated at $\hat{x}_1 = -0.05$. It is expected that the influence on the near-tip elements and fracture process zone of any marginally active elements that may have been deleted is negligible.

A CRITERION FOR DUCTILE STABLE CRACK GROWTH

The computational results for the steadily propagating plane strain tensile crack with fracture process zone can be used to clarify the fracture criterion proposed by Rice and Sorenson (1978). These authors suggest that continuing ductile stable crack propagation is characterized by the attainment of a critical crack opening displacement at a characteristic material distance behind the advancing crack tip. The characteristic material distance in this crack growth criterion can be identified with the size of the fracture process zone.

The calculations for the planar slip element mesh with fracture process zone indicate that the elements adjacent to the crack tip play an increasingly dominant role in the elastic singularity cancellation when they are refined to smaller and smaller sizes. This trend is manifested by the fact that the computed fracture process zone size becomes smaller and smaller with increasingly refined near-tip element meshes. The true fracture process zone size will be the value that is obtained in the limiting case of an infinitely refined mesh of elements adjacent to the crack tip.

The relationship between fracture process zone size and crack tip element area is illustrated in Fig. 7. The plot has been constructed using computed fracture process zone size results from four successive refinements of the elements adjacent to the crack tip. Fitting a Lagrange interpolating polynomial to the data points and extrapolating to zero crack tip element area leads to an estimate of

$$x^* = 0.000601 \frac{K^2}{\tau_0^2} \tag{53}$$

for the true size of the fracture process zone. This confirms the prediction of Rice and Sorenson (1978) that the size of the fracture process zone under conditions of small-scale yielding and plane strain is exceedingly small. The result of equation (53) can be contrasted with Dugdale's strip-yielding zone size of $x^* = (\pi/24)(K^2/\tau_0^2)$ for conditions of small-scale yielding and plane stress.

The fracture criterion given by Rice and Sorenson (1978) can be stated in the form

$$\frac{\delta_0}{x^*} = \left(\frac{\delta_0}{x^*}\right)_{\text{crit}}. \tag{54}$$

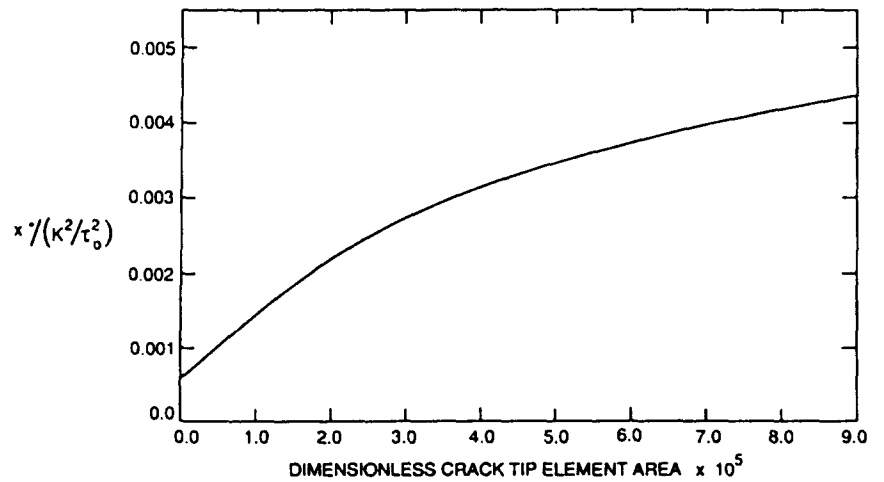

Fig. 7. Determination of true fracture process zone size.

which implies that the ratio of the crack tip opening displacement δ_0 to the fracture process zone size x^* attains a constant critical value during crack propagation. This critical value depends only on material properties. Equation (54) can also be interpreted as a statement that ductile crack growth is characterized by an invariant crack tip opening angle. For this reason, the relationship is often referred to as the critical crack tip opening angle criterion.

In the model of the steadily propagating plane strain tensile crack developed in this work, δ_0 is the crack tip opening displacement calculated from eqn (52) and x^* is the computed fracture process zone size. Using the same four element meshes employed in the estimate of the true fracture process zone size, the ratio δ_0/x^* was found to be nearly invariant with respect to near-tip element mesh refinement. The constant value of δ_0/x^* during mesh refinement establishes the accuracy of the crack tip opening angle result obtained in this paper. Taking the mean value from the four element meshes and using dimensioned variables, this result can be expressed as

$$\frac{\delta_0}{x^*} = 13.316\frac{\tau_0}{E}, \tag{55}$$

where Young's modulus $E = 2\mu(1+\nu)$ and Poisson's ratio $\nu = 1/2$. The maximum deviation from this result amongst the four element meshes considered is less than 6%.

Rice and Sorenson (1978) have interpreted the data of Clark *et al.* (1978) in terms of the critical crack tip opening angle criterion. The results were obtained from crack growth tests in small fully plastic bend specimens of pressure vessel steels. For the entire group of materials tested, values ranging from $\delta_0/x^* = 9.89(\tau_0/E)$ to $\delta_0/x^* = 534.0(\tau_0/E)$ were observed. The numerically calculated result of eqn (55) falls into the lower end of this range. Although the test results of Clark *et al.* (1978) are representative of the initial stage of crack growth under large-scale yielding conditions, this agreement indicates that the fracture process zone model described in this paper gives physically reasonable values of the crack tip opening angle.

CONCLUSIONS

The numerical study of the fracture process zone near the tip of a steadily propagating plane strain tensile crack suggests the following conclusions.

(1) The influence of the fracture process zone is confined to the deformation field close to the crack tip. Inside this region, the fracture process zone removes the crack tip plastic strain singularity which is present in models that do not account for the failure of the material at the crack tip. Outside this region, the macroscopic plastic zone possesses features revealed by earlier investigations of plane strain tensile crack growth.

(2) The size of the fracture process zone ahead of the propagating crack decreases with refinement of the near-tip element mesh. A small but appreciable fracture process zone remains when the area of the elements adjacent to the crack tip is extrapolated to zero. The size of the fracture process zone for a moving crack with a macroscopic plastic zone in the vicinity of the crack tip is two orders of magnitude smaller than the classical Dugdale fracture process zone size based on the elastic deformation of the crack.

(3) The numerical results for crack tip opening displacement and fracture process zone size can be employed to obtain an accurate estimate of the critical crack tip opening angle associated with ductile stable crack growth. The numerically calculated crack tip opening angle is found to be physically reasonable when compared with the results of crack growth tests in pressure vessel steels.

Acknowledgements — The author wishes to express his sincere gratitude to Professor N. C. Huang of the University of Notre Dame for helpful guidance throughout the course of this project. The author also wishes to thank his mother, Mrs D. G. Russell, for her invaluable assistance in the preparation of the revised version of the manuscript.

REFERENCES

Achenbach, J. D. and Dunayevsky, V. D. (1984). Crack growth under plane stress conditions in an elastic-perfectly plastic material. *J. Mech. Phys. Solids* **32**, 89–100.

Aravas, N. and McMeeking, R. M. (1985). Microvoid growth and failure in the ligament between a hole and a blunt crack tip. *Int. J. Fract.* **29**, 21–38.

Bilby, B. A., Cottrell, A. H. and Swinden, K. H. (1963). The spread of plastic yield from a notch. *Proc. R. Soc. Lond.* **A272**, 304–314.

Budiansky, B. and Hutchinson, J. W. (1978). Analysis of closure in fatigue crack growth. *J. Appl. Mech.* **45**, 267–276.

Chitaley, A. D. and McClintock, F. A. (1971). Elastic-plastic mechanics of steady crack growth under anti-plane shear. *J. Mech. Phys. Solids* **19**, 147–163.

Clark, G., El Soudani, S. M., Ferguson, W. G., Smith, R. F. and Knott, J. W. (1978). Ductile crack extension in pressure vessel steels. *Conf. on Tolerance of Flaws in Pressurized Components*, Institution of Mechanical Engineers, London.

Dean, R. H. and Hutchinson, J. W. (1980). Quasi-static steady crack growth in small-scale yielding. *Fracture Mechanics: Twelfth Conf.*, American Society for Testing and Materials, ASTM STP 700, 383–405.

Denda, M. (1983a). A dislocation approach to steady crack growth. Report MECH-46, Division of Applied Sciences, Harvard University.

Denda, M. (1983b). A dislocation approach to steady crack growth. Ph.D. thesis, Division of Applied Sciences, Harvard University.

Denda, M. (1986). Formulation of the plastic source method for plane inelastic problems, part I: Green's functions for plane inelastic deformations. Technical Report, Department of Mechanics and Materials Science, Rutgers University.

Denda, M. and Lua, Y. J. (1986). Formulation of the plastic source method for plane inelastic problems, part 2: numerical implementation for plane elastoplastic problems. Technical Report, Department of Mechanics and Materials Science, Rutgers University.

Drugan, W. J. (1986). Radial dependence of near-tip continuum fields for plane strain tensile crack growth in elastic ideally plastic solids. *J. Appl. Mech.* **53**, 83–88.

Drugan, W. J., Rice, J. R. and Sham, T. L. (1982). Asymptotic analysis of growing plane strain tensile cracks in elastic ideally plastic solids. *J. Mech. Phys. Solids* **30**, 447–473.

Dugdale, D. S. (1960). Yielding of steel sheets containing slits. *J. Mech. Phys. Solids* **8**, 100–108.

Elber, W. (1970). Fatigue crack closure under cyclic tension. *Engng Fract. Mech.* **2**, 37–45.

Eshelby, J. D. (1957). The determination of the elastic field of an ellipsoidal inclusion, and related problems. *Proc. R. Soc. Lond.* **A241**, 376–396.

Narasimhan, R., Rosakis, A. J. and Hall, J. F. (1987a). A finite element study of stable crack growth under plane stress conditions: part I—elastic perfectly plastic solids. *J. Appl. Mech.* **54**, 838–845.

Narasimhan, R., Rosakis, A. J. and Hall, J. F. (1987b). A finite element study of stable crack growth under plane stress conditions: part II—influence of hardening. *J. Appl. Mech.* **54**, 846–853.

Needleman, A. and Tvergaard, V. (1987). An analysis of ductile rupture modes at a crack tip. *J. Mech. Phys. Solids* **35**, 151–183.

Ponte Castañeda, P. (1986). Asymptotic fields of a perfectly-plastic, plane stress, mode II growing crack. *J. Appl. Mech.* **53**, 831–833.

Ponte Castañeda, P. (1987a). Asymptotic fields in steady crack growth with linear strain-hardening. *J. Mech. Phys. Solids* **35**, 227–268.

Ponte Castañeda, P. (1987b). Asymptotic analysis of a mode I crack propagating steadily in a deformation theory material. *J. Appl. Mech.* **54**, 79–86.

Rice, J. R. (1967). Mechanics of crack tip deformation and extension by fatigue. *Fatigue Crack Propagation*, American Society for Testing and Materials, ASTM STP 415, 247–311.

Rice, J. R. (1968). Mathematical analysis in the mechanics of fracture. In *Fracture—An Advanced Treatise* (Edited by H. Liebowitz), Vol. II, pp. 191–308. Academic Press, New York.

Rice, J. R. (1982). Elastic–plastic crack growth. *Mechanics of Solids, the Rodney Hill 60th Anniversary Volume* (Edited by H. G. Hopkins and M. L. Swell), pp. 539–562. Pergamon Press, Oxford/New York.

Rice, J. R., Drugan, W. J. and Sham, T. L. (1980). Elastic–plastic analysis of growing cracks. *Fracture Mechanics: Twelfth Conf.* American Society for Testing and Materials, ASTM STP 700, 189–221.

Rice, J. R. and Sorenson, E. P. (1978). Continuing crack tip deformation and fracture for plane strain crack growth in elastic–plastic solids. *J. Mech. Phys. Solids* **26**, 163–186.

Russell, S. G. (1987). Application of dislocation theory to crack growth problems. Ph.D. thesis, Department of Aerospace and Mechanical Engineering, University of Notre Dame.

Sham, T. L. (1983). A finite element study of the asymptotic near-tip fields for mode I plane strain cracks growing stably in elastic ideally plastic solids. *Elastic–Plastic Fracture: Second Symp., Vol. I—Inelastic Crack Analysis*, American Society for Testing and Materials, ASTM STP 803, 52–79.

Slepyan, L. I. (1974). Growing crack during plane deformation of an elastic–plastic body. *Mekhanika Tverdogo Tela* **9**, 57–67.

Sorenson, E. P. (1979). A numerical investigation of plane strain stable crack growth under small-scale yielding conditions. *Elastic–Plastic Fracture*, American Society for Testing and Materials, ASTM STP 668, 151–174.

Weertman, J. (1978). Fatigue crack propagation theories. *Fatigue and Microstructure*, American Society for Metals, 279–306.

Wnuk, M. P. (1974). Quasi-static extension of a tensile crack contained in a viscoelastic–plastic solid. *J. Appl. Mech. Trans. ASME, Series E* **41**, 231–242.

Wu, K. C. and Hui, C. Y. (1987a). A complex-variable method for two dimensional internal stress problems and its applications to crack growth in nonelastic materials: part I—theory. *J. Appl. Mech.* **54**, 59–64.

Wu, K. C. and Hui, C. Y. (1987b). A complex-variable method for two dimensional internal stress problems and its applications to crack growth in nonelastic materials: part II—applications. *J. Appl. Mech.* **54**, 65–71.